Effects of Convection and Microwave Drying Schemes on the Characteristics and Sound Absorption of Acoustic Oil Palm Boards

Panya Dangvilailux and Jarruwat Charoensuk *

This research aimed to develop economical, high-performance acoustic oil palm boards (OPB) using the convection (CV) and microwave (MW) wood drying technologies under variable thermal conditions. The results revealed that the CV and MW oven temperatures were positively correlated with moisture desorption but inversely correlated with drying time. The CV heating temperatures were inversely and positively correlated with the density and volumetric shrinkage, respectively, and the MW power output was positively correlated with density and shrinkage. Thus, the MW-treated OPB specimens exhibited stronger mechanical characteristics than the CV-treated OPB specimens. Importantly, the CV-treated OPB specimens acoustically outperformed the MW-treated counterparts, as evidenced by the former's higher noise reduction coefficients (NRC). This phenomenon was attributed to the abundance of fissures between the vascular bundles and the parenchyma. Thus, the CV technology was more operationally and economically suited to the high-performance acoustic OPB.

Keywords: Convective drying; Microwave drying; Oil palm board; Sound absorption coefficient; Noise reduction coefficient

Contact information: Department of Mechanical Engineering, Faculty of Engineering, King Mongkut's Institute of Technology Ladkrabang, Bangkok 10520, Thailand;
** Corresponding author: jarruwat.ch@kmitl.ac.th*

INTRODUCTION

Oil palm trees (*Elaeis guineensis* Jacq.), which belong to the Liliopsida class (monocotyledonous) of the Arecaceae family (Moreno and Romero 2015), are an important economic crop, especially the palm oil, which is processed into edible oils and biofuels (Sanderson 2011; Johari *et al.* 2015). According to Potts *et al.* (2014), Indonesia, Malaysia, and Thailand collectively account for a large proportion of global oil palm cultivation. The economic lifespan of an oil palm tree is 25 years, after which the yields decrease significantly, and the tree height presents an operational challenge to the oil palm growers (*i.e.*, difficulty harvesting the fruits). The oil palm trees are thus typically felled once the retirement age is reached.

According to Erwinsyah (2008), felled oil palm trees generated roughly 20 million m^3 of oil palm biomass globally. The oil palm trunks (OPT), which are high in moisture (70% to 80% wet basis) with 65% to 80% holocellulose and 18% to 21% lignin, generate a particularly large amount of oil palm biomass (Hng *et al.* 2011). Currently, oil palm trunks are processed and used independently or collectively in the production of paper products, bio-composites, reconstituted boards, plywood, cement-bonded particleboard, and medium-density fiberboard (MDF) (Schwarz 1985; Teck and Ong 1985; Choon *et al.* 1991; Subiyanto *et al.* 2002; Sulaiman *et al.* 2012; Nadhari *et al*. 2013).

Commonly used hardwood and softwood drying technologies include the solar kiln drying (Langrish 2013), convective drying (Ouertani *et al*. 2015), microwave drying (Vongpradubchai and Rattanadecho 2011; Abdul Khalil *et al.* 2012; Lai and Idris 2013), radio frequency vacuum drying (Elustondo *et al*. 2004; Jung *et al*. 2004), and freeze drying methods (Bhattacharya *et al*. 2014). These drying methods are diverse in their operational complexity and investment cost. Thus, operational requirements, costs, and benefits should be taken into consideration in the selection and adoption of a wood-drying technology. Given the unique nature of oil palm trunks, this experimental research adopted the convection (CV) and microwave (MW) drying technologies. MW drying consumes 50% less energy and produces substantially less volatile organic compounds emissions, compared to the CV drying method (Du *et al*. 2005). Furthermore, due to the minimal operational complexity and subsequent maintenance costs of both technologies, the end product (*i.e.*, oil palm acoustic board) would be more affordable at the commercialization stage. More importantly, the conversion from oil palm trunks to acoustic boards would be a boon to the environment, as the open burning of retired oil palm trees could be somewhat averted. Given high toxicity of fibrous rock/glass and foam plastics in the conventional acoustic boards (Asdrubali 2006), OPB is thus a greener and more environmentally sustainable alternative.

According to Arenas and Crocker (2010), sound barrier materials should absorb most sound energy and reflect minimal noise. Previous research on sound (acoustic) absorption materials using agricultural waste materials included acoustic materials fashioned from naturally-dried coir fibers (Fouladi *et al.* 2011), pure *Arenga pinnata* dried fibers (Ismail *et al.* 2010), oil palm mesocarp (Latif *et al*. 2015), oil palm empty fruit bunch (Or *et al*. 2016; Or *et al*. 2017), and perforated oil palm trunk treated with infrared (Kerdtongmee *et al.* 2016).

This research aims to develop economical and high-performance acoustic oil palm boards (OPB) using retired oil palm trunks. To that end, the convection (CV) and microwave (MW) wood drying technologies were deployed, and the hot-air temperatures and microwave power outputs were varied between 50 °C, 60 °C, 80 °C, and 100 °C and 100 W, 400 W, 1200 W, and 4000 W, respectively. In CV drying, moisture is transported to the surface mainly due to capillary forces where evaporation occurs. The demarcation between the dry zone and an inner moist zone moves toward the center of the wood during convective drying. Meanwhile, previous research on MV drying has experimented with OPT using an input power range of 660 to 3300 W (Amouzgar *et al*. 2010; Abdul Khalil *et al*. 2012). In MW drying, the MW absorption is initially high, as evidenced by elevated drying rates, and decreases as large volumes of moisture (*i.e.* dielectric) are expelled. The CV-treated and MW-treated OPB specimens were subsequently assessed in terms of their drying kinetics (moisture-temperature kinetics relative to time), physical and mechanical properties, and sound absorption performance.

EXPERIMENTAL

The anatomical structure of OPT consists of hardwoods (vascular bundles and parenchyma cells) and softwoods (cells of fibers, tracheids, vessels parenchyma, and ray parenchyma cells) (Sulaiman *et al*. 2012), as shown in Fig. 1. The average population of vascular bundles at the inner is 26 vascular bundles/cm^2 and the fiber has the average

dimensions of about 30 μm in diameter and 1.24 mm in length (Erwinsyah 2008). The experimental oil palm trees were the cultivar Tenera from a plantation in Thailand's southern province of Chumphon. The trees were 26 years old and thus were push-felled, given their normal retiring age of 25 years. To obtain homogeneous vascular bundles and density, the felled trees were cut into stumps of 2 m in height (length) measuring from the trunk base prior to transformation into OPT discs.

The transversal-cut OPT discs were 50 to 65 cm in diameter and 20 mm in thickness, with an initial moisture content of 287% ± 0.5% dry basis (db). The discs were soaked in hot water at 85 °C for 20 min prior to centrically processing into pre-thermally treated oil palm boards (OPB) with 200 mm × 200 mm × 20 mm (W × L × T) in dimension. Specifically, the pre-treated OPB was extracted from the OPT center, given the low density suitable for sound absorbing applications, and underwent the non-chemical hot water process to remove abundant glucose and other fermentable sugars in the sap and prevent mold growth. Prior to the thermal treatment, the temperature and moisture content of the fresh OPBs were maintained at 28 °C and 350% ± 2.7% (db). The density of the soaked OPB specimens was in the range of 1000 to 1,100 kg/m^3. Four experimental OPB specimens were fabricated under each thermal condition: 50 °C, 60 °C, 80 °C, and 100 °C CV temperatures and 100 W, 400 W, 1200 W, and 4000 W MW power outputs, producing a total of 32 OPB specimens. Each OPB specimen was placed 200mm apart from one another and 200 mm from the chamber walls.

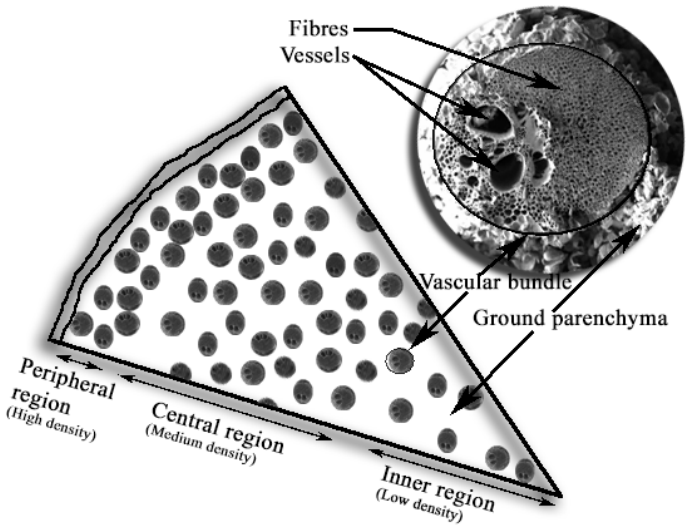

Fig. 1. Cross-section of oil palm trunk

The geometry of the experimental convection-microwave drying system was as follows: the drying chamber had dimensions of 1000 mm × 1000 mm × 500 mm (W × L × H), was composed of stainless steel type 316, and was outfitted with one convective electrical heater and four microwave magnetrons. The heater had a maximum power output of 5000 W and was thermostat-controlled, with a blower to generate an air speed of 2.00 m/s. Inlet drying air and OPB were measured by thermocouples (Type K, Chromel–Alumel) connected to a data logger with an accuracy of ±2 °C. The temperatures of thermally-treated OPB specimens were taken at a 10 mm depth at the four corners and center of the specimens and averaged. The in-chamber microwave power was 100 to 4000

W (2450 MHz) using waveguides. In addition, a circulating low-speed fan was used to evenly distribute the in-chamber hot air and microwave energy.

The hot-air temperatures and microwave power outputs (*i.e.*, the thermal conditions) were varied between 50 °C, 60 °C, 80 °C, and 100 °C and 100 W, 400 W, 1200 W, and 4000 W, respectively. The heating cycles were terminated once the moisture content reached an equilibrium moisture of 10% ± 2% db (from originally 350 % ± 2.7% db).The effects of the convection (CV) and microwave (MW) drying technologies under variable thermal conditions (50 °C, 60 °C, 80 °C, and 100 °C and 100 W, 400 W, 1200 W, and 4000 W) on the OPB specimens were determined with regard to drying kinetics (moisture-temperature kinetics relative to time), physical and mechanical properties, and sound absorption performance. Specifically, the analysis of the OPBs' physical properties, including oven-dry density, volumetric shrinkage, and color, was carried out in accordance with ASTM D2395-14. The mechanical properties were determined according to ASTM D143-14, including tension strength perpendicular to grain (using 5x20x200mm samples at a cross-head speed of 1.0 mm/min), compression strength parallel to grain (using 20x20x100mm samples at a cross-head speed of 0.3 mm/min), shear strength parallel to grain (using 20x20x60mm samples at a cross-head speed of 0.6 mm/min), static bending (using 20x20x200mm samples at a cross-head speed of 1.3 5 mm/min), and hardness (using 50x20x150mm samples at a cross-head speed of 6 mm/min with a 10 mm (diameter) ball). Furthermore, scanning electron microscopy (SEM) was used to determine the morphology and sound absorption performance of the OPB specimens.

In this research, the moisture content (*M*) and the moisture content ratio (*MR*) were calculated with Eq. 1 and Eq. 2, respectively (Ouertani *et al*. 2015).

$$M(\%) = \frac{M_{ini} - M_o}{M_o} \times 100 \quad (1)$$

$$MR = \frac{M}{M_{ini}} \quad (2)$$

where M is the average moisture content of the specimen at the time of the test (kg water/ kg dry mass), M_{ini} is the initial mass, and M_o is the oven-dry mass.

The oven-dry density (ρ_o) was calculated as,

$$\rho_o = \frac{M_o}{V_o} \quad (3)$$

where M_0 is the oven-dry mass and V_o is the oven-dry volume of the specimen (m^3).

The volumetric shrinkage (S_v) was calculated as,

$$S_v(\%) = \frac{V_g - V_o}{V_g} \times 100 \quad (4)$$

where V_g is the volume of specimen in fresh (pre-thermally treated) condition and V_o is the oven-dry volume of the specimen (m^3) in the x, y, and z directions.

In the color analysis, measurements were first taken on the individual OPB specimens (32 specimens) at five locations (the center and each of the four corner-edges) using the Minolta CR-400 Chroma Meter (Konica Minolta Sensing, Inc., Osaka, Japan). The measurements associated with each thermal condition were then summed and averaged. The results were expressed as the whiteness/blackness (L^*), redness/greenness (a^*), yellowness/blueness (b^*) and hue angle (Hue).

The mechanical properties of the thermally treated OPB specimens were assessed with regard to the tension strength perpendicular to grain, compression strength parallel to grain, shear strength parallel to grain, static bending, and hardness. The measurements were taken using a texture analyzer (TA Plus texture analyzers, Lloyd Instruments, West Sussex, England) with a 1 kN static load cell.

The morphology and acoustic (sound-absorbing) performance of the CV-treated and MW-treated OPB specimens under variable thermal conditions were analyzed by scanning electron microscopy (SEM) with a 50x magnification and a 10 kV accelerating voltage (ZEISS-MERLIN Compact, Oberkochen, Germany).

The sound absorption coefficients (SAC) of the thermally-treated OPB specimens (Fig. 2) were determined *via* the impedance tube method in accordance with ISO 10534-2, using two tube sizes of 30 mm and 100 mm in diameter (Sa'adon 2015). The smaller tube was used for absorption testing at high frequency (1000 Hz to 6400 Hz) and the larger tube was used for absorption testing at low frequency (0.0 Hz to1000 Hz). The noise reduction coefficients (NRC) of the OPB specimens under both drying technologies were determined according to the ASTMC423-09 standard, whereby the NRC is the average value of the sound absorption coefficients (SAC) at 250 Hz, 500 Hz, 1000 Hz, and 2000 Hz, where α_i is the sound absorption coefficient for that particular frequency. The NRC values of the OPB specimens were calculated with Eq. 5:

$$NRC = \frac{[(\alpha_{250} + \alpha_{500} + \alpha_{1,000} + \alpha_{2,000})]}{4} \quad (5)$$

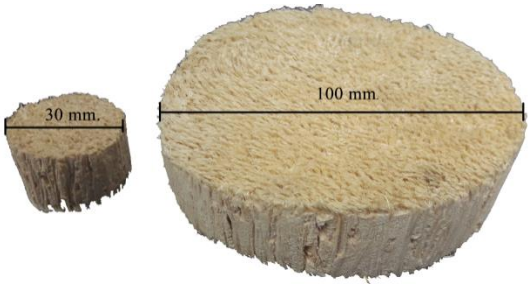

Fig. 2. The diameter of OPB specimens as determined by the impedance tube method at 30 mm and 100 mm

RESULTS AND DISCUSSION

The OPB Drying-temperature Kinetics

As previously stated, the pre-thermally treated moisture content and temperature of the OPB specimens were 350% ± 2.7% (db) and 28 °C, and the target moisture content was 10% ± 2% db. Figure 3a illustrates the moisture-temperature kinetics relative to time associated with the convection (CV) drying scheme under the 50 °C, 60 °C, 80 °C, and 100 °C thermal conditions. Under the 50 °C condition, the target moisture content of 10% ± 2% db was achieved after 4000 min with an average OPB temperature of 41.6 °C. Meanwhile, the heating cycle was terminated after 1690 min and 700 min with the OPB temperatures of 46.2 °C and 58.3 °C under the 60 °C and 80 °C conditions, respectively. Under the 100 °C condition, the target moisture content was reached after 480 min with an

OPB temperature of 62.1 °C. The findings indicated that heating temperature was positively correlated with moisture desorption rate but inversely correlated with drying time. In other words, the higher the heating temperature, the more efficient the moisture expulsion and the shorter the drying period. At 80 and 100° C CV drying, moisture is transported to the surface where evaporation occurs. The internal moisture content decreases with elongated drying time, generating numerous pores of variable sizes.

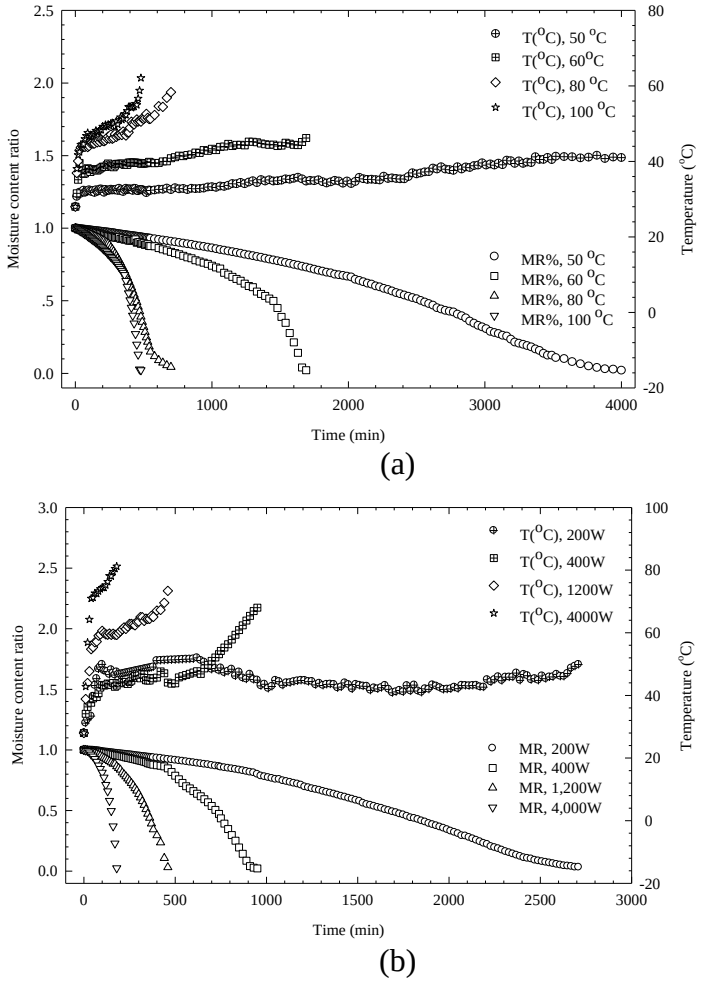

Fig. 3. The moisture-temperature kinetics relative to time: (a) convection drying schemes (b) microwave drying schemes

Figure 3b depicts the moisture-temperature kinetics relative to time of the microwave (MW) drying scheme under the 200 W, 400 W, 1200 W, and 4000 W thermal conditions. Under the 200 W MW condition (the lower extreme), the target moisture content was reached after 2770 min with an OPB temperature of approximately 50 °C. Under the 4000 W condition (the upper extreme), the MW heating was terminated after 180 min with an OPB temperature of 81.2 °C. Under the 400 W and 1200 W conditions, the heating was terminated after 950 min and 450 min with the OPB temperatures of 67.9 °C and 73.4 °C, respectively. By comparison, the MW drying periods both the extreme and moderate conditions were considerably shorter than those of the CV scheme. This finding could be attributed to internal heat generation resulting from MW-induced mass transfer and subsequent rapid moisture desorption. Given the high moisture content of the OPB

specimens, the microwave energy was effectively absorbed and converted into sensible heat. The uneven internal wood temperature was induced by the electromagnetic field distribution and the power penetration depth, *i.e.*, the higher the MW output power, the less the power penetration (Lars 2007).

Further analysis revealed that the relative dielectric constant (ε'), the loss factor (ε''), and the loss tangent (tanδ) of the pre-treated OPB specimens (*i.e.* the fresh OPB) were 5.61, 0.96, and 0.17, respectively, given the average 2250 MHz resonant frequency, using the Dielectric Measurement kit μWaveAnalyser of PÜSCHNER Microwave Power Systems. Given the high loss factor (ε'') of 0.96 of the fresh OPB specimens, the microwave energy was almost completely absorbed by the specimens over the course of thermal treatment. Nonetheless, the microwave absorption decreased with time as the moisture content decreased, as shown in Fig. 3b. The MW-induced internal heat generation contributes to accumulative internal pressures, which in turn enables the pressure-driven moisture migration. As the moisture decreases, the loss factor and drying-rate ratio decrease. According to Feng *et al*. (2001), the electromagnetic field contributed to the vibration of water molecules and the subsequent changes in the configuration of the electric field in the wood.

Physical Properties of OPB

Table 1 compares the physical characteristics at the target moisture content of 10% ± 2% db of the OPB specimens associated with the convection (CV) and microwave (MW) drying schemes under variable thermal conditions. Under the CV scheme, the heating temperatures were strongly inversely correlated with oven-dry density and positively associated with volumetric shrinkage. Specifically, with increase in temperature from 50 °C (lower extreme) to 100 °C (upper extreme), OPB density decreased from 265 kg/m^3 to 247 kg/m^3 as fissures developed between the OPB vascular bundles and the parenchyma tissues, and the volumetric shrinkage increased from 15.42% to 23.94%. In addition, the OPB color changed as *L** decreased from 82.8 to 71.72, *a** increased from 1.77 to 6.49, *b** increased from 22.61 to 27.01, and Hue decreased from 87.31 to 76.48. The color of the OPB became light reddish with increased heating temperature, whereas the color of the pre-treated (fresh) OPB was yellowish (Table 1).

Table 1. Comparison of the Physical Characteristics of the OPB Specimens of the Convection and Microwave Drying Schemes under Variable Thermal Conditions

Drying Treatment		Oven-dry Density (kg/m^3)	Volumetric Shrinkage (%)	*L**	*a**	*b**	Hue
Convection	50 °C	265	15.42	82.8	1.77	22.61	87.31
	60 °C	262	18.38	77.76	1.15	24.51	85.53
	80 °C	259	21.92	77.64	3.11	21.27	81.68
	100 °C	247	23.94	71.72	6.49	27.01	76.48
Microwave	200W	352	44.42	79.5	1.69	21.50	85.5
	400W	385	48.72	75.17	3.80	21.49	79.98
	1200W	416	53.69	59.01	6.15	25.06	76.20
	4000W	458	65.90	48.58	6.19	21.55	73.97
OPB Specimen		900 to 1100		70.55	1.88	26.13	85.88

Essentially, the higher convection oven temperatures contributed to a more rapid desorption rate, a lower density, and a higher volumetric shrinkage. Under the microwave drying scheme, the moisture desorption was substantially accelerated as a result of the MW-induced mass transfer and subsequent internal heat generation. The MW power output was positively correlated with the oven-dry density and volumetric shrinkage of the OPB specimens. The OPB density and the volumetric shrinkage rose from 352 kg/m^3 to 485 kg/m^3 and from 44.42% to 65.90% under the 200 W (lower extreme) and 4000 W (upper extreme) conditions, respectively.

The greater density was attributed to the MW-induced excitation of parenchyma tissues and the subsequent higher shrinkage and greater compactness of the MW-treated OPB specimens. As moisture is expelled from the product, a pressure imbalance (*i.e.* variation in pressure between the inner of the material and the external pressure) occurs, producing contracting stresses that lead to material shrinkage or breakdown and deformation. Moreover, the OPB color changed from yellowish to brownish with sporadic burn marks, corresponding to a decrease in brightness (Table 1).

Mechanical Properties of OPB

Table 2 presents the mechanical properties, including the tension strength perpendicular to grain, compression strength parallel to grain, shear strength parallel to grain, static bending, and hardness, at the target moisture content of 10 ± 2% db of the OPB specimens associated with the convection (CV) and microwave (MW) drying schemes under variable thermal conditions. Specifically, under the CV scheme, the tension strength perpendicular to grain, compression strength parallel to grain, shear strength parallel to grain, static bending, and hardness decreased as the hot-air temperatures increased.

Table 2. Comparison of the Mechanical Properties of the OPB Specimens Associated with the Convection and Microwave Drying Schemes under Variable Thermal Conditions

Drying Treatment		Tension (MPa)	Compression (MPa)	Shear Strength (MPa)	Static Bending		Hardness Strength (kg)
					MOR (MPa)	MOE (MPa)	
Convection	50 °C	0.2282	0.4108	0.4464	19.584	1145.457	43.1
	60 °C	0.2035	0.3833	0.4226	14.761	933.315	37.8
	80 °C	0.1788	0.2249	0.4026	12.146	904.727	19.5
	100 °C	0.1463	0.1713	0.2884	6.591	698.809	13.6
Microwave	200 W	0.2538	0.6226	0.5038	30.321	1163.098	22.8
	400 W	0.2819	0.7849	0.5174	31.459	1566.011	42.1
	1200 W	0.3347	0.9610	0.5302	32.529	2758.088	49.5
	4000 W	0.4222	1.5690	0.6640	76.840	8550.933	65.9

In contrast, under the MW scheme, mechanical strength increased with increasing MW power outputs. This observation was consistent with the increased shrinkage and density as MW power increased. By comparison, the MW-treated OPB specimens exhibited stronger mechanical characteristics than those of the CV scheme.

Morphology and Scanning Electron Micrographs

Figures 4 and 5, respectively, illustrate the cross-sectional areas of the CV-treated and MW-treated OPB specimens under various thermal conditions. In Fig. 4, under the CV scheme, the abundance of pores and fissures and the heating temperature were positively related. Specifically, at 100 °C, the OPB specimens became visibly porous with the presence of numerous cavities of 5mm to 10 mm in diameter (Fig. 4d), vis-à-vis under the lower hot-air temperatures (Figs.4a-c).

In Fig. 5, under the MW drying scheme, the OPB specimens exhibited no cavity and became denser as the MW power output increased. In addition, at 4000 W, sporadic burn marks (hotspots) were observed (Fig. 5d) corresponding to the highest shrinkage ratio. By comparison, the density of the 4000W MW specimen was increased by about 10% and also the mechanical properties enhanced, compared with the 1200W MW specimen. Given that the hotspots on the 4000W MW specimen possess poor mechanical strength, measurements were thus carried out at non-hotspot areas.

Figure 6 illustrates the SEM images of the CV-treated OPB specimens under the various hot-air temperatures of 50 °C, 60 °C, 80 °C, and 100 °C. As heating temperatures increased, fissures developed between the vascular bundles and parenchyma cells of the OPB specimens, which was most pronounced in Fig. 6(d).

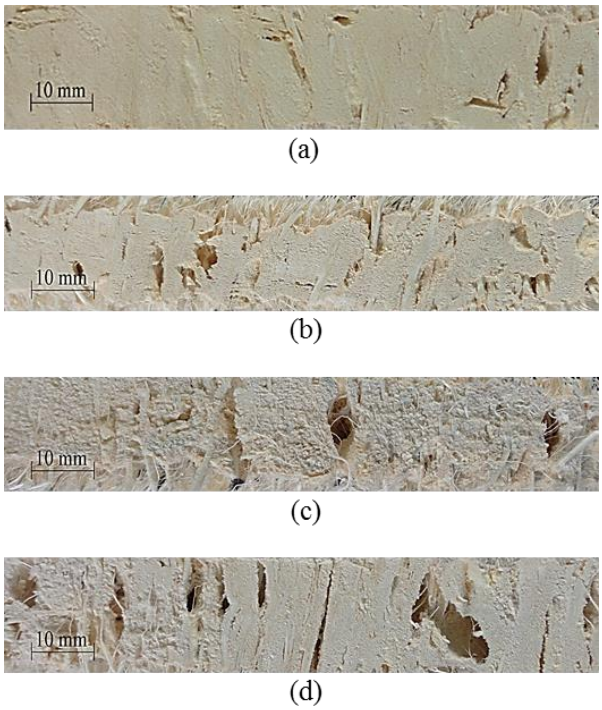

Fig. 4. The cross-sectional view of the CV-treated OPB specimens at (a) 50 °C, (b) 60 °C, (c) 80 °C, and (d) 100 °C

Figure 7 depicts the SEM images of the MW-treated OPB specimens under the various microwave power outputs of 200 W, 400 W, 1200 W, and 4000 W. Interestingly, no fissure emerged in the MW-treated OPB specimens as the microwave power output increased. In fact, the vascular bundles and parenchyma cells became denser as MW power output increased.

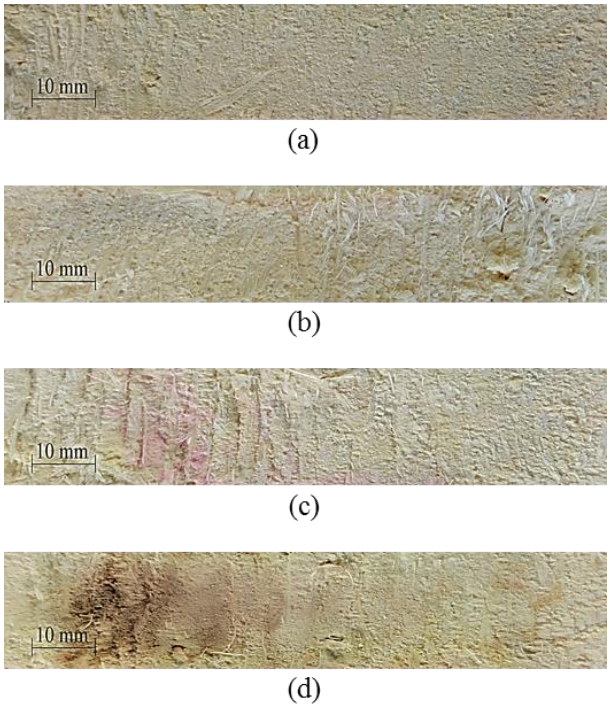

Fig. 5. The cross-sectional view of the MW-treated OPB specimens at (a) 200 W, (b) 400 W, (c) 1200 W, and (d) 4000 W

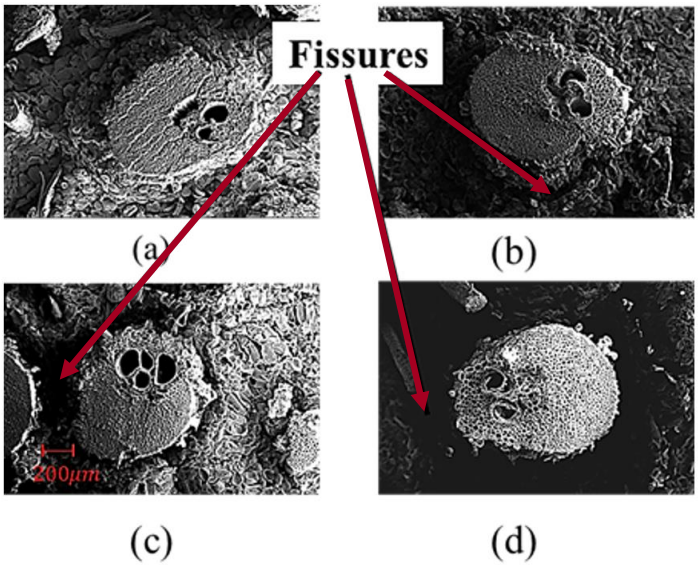

Fig. 6. SEM images of the vascular bundles and the parenchyma tissues of the CV-treated OPB specimens at (a) 50 °C, (b) 60 °C, (c) 80 °C, and (d) 100 °C

Sound Absorption Coefficient (SAC)

Figure 8a illustrates the sound absorption coefficient (SAC) of the CV-treated specimens. In the figure, the substantially high SACs were realized at around 500 Hz and 2000 Hz. The first peak was attributable to abundant vascular bundles, fissures and cavities (Helmholtz resonator) while the second peak to abundant fibers and porosity. Figure 8b illustrates the SAC of the MW-treated OPB specimens. Due to very high density of the

MW specimens, the highest SAC was achieved once in the 500 to 1000 Hz frequency range, depending on MW output power.

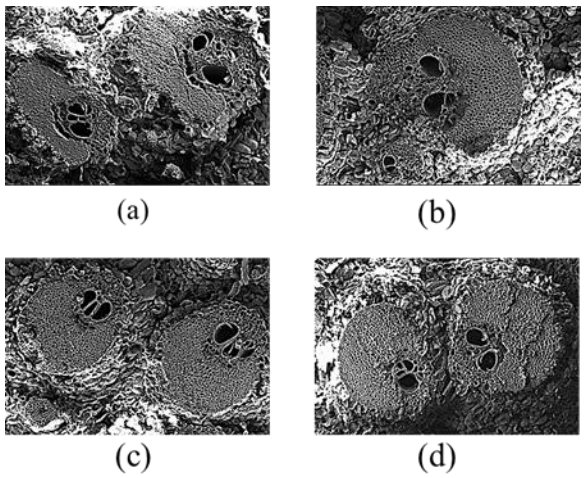

Fig. 7. SEM images of the vascular bundles and the parenchyma tissues of the MW-treated OPB specimens at (a) 200 W, (b) 400 W, (c) 1200 W, and (d) 4000 W

Table 3 tabulates the maximum SACs and the noise reduction coefficients (NRC) of the OPB specimens. NRC is the average of the sound absorption coefficients (SAC) at 250 Hz, 500 Hz, 1000 Hz, and 2000 Hz. The NRCs of the CV-treated specimens were higher than those of the MW-treated specimens due to the former's abundant surface-fissures and internal cavities. The CV-treated OPB specimens acoustically outperformed the MW-treated counterparts as evidenced by the former's higher NRCs under all thermal conditions. This phenomenon could be attributed to the abundance of fissures between the vascular bundles and the parenchyma in the CV-treated OPB specimens, which in turn contributed to better sound absorption performance. In fact, as the vascular bundles were considerably stronger than the parenchyma cells, the hot air accelerated the water desorption of the parenchyma and the vascular bundles acted as a piping network to transfer the internal water to the specimen surface.

In addition, the NRCs associated with the microwave drying technology were lower than those of the convection scheme. These results could be explained by the OPB's characteristic vascular bundles embedded in the parenchyma tissues. Thus, at a sufficiently high shrinkage ratio, the stress on the parenchyma is transferred to the vascular bundles, strengthening the OPB. In addition, the very high porosity of the parenchyma, particularly in the fresh (pre-thermally treated) condition, enables it to absorb large quantities of water vis-à-vis the vascular bundles (Norralakmam 2007; Abdullah *et al*. 2012). Once the parenchyma tissues were dehydrated and uniformly shrunk with the vascular bundle, a dense material was formed.

According to Cowan (1994), an acoustic material whose NRC is in excess of 0.4 is regarded as a high-quality, high-performance acoustic material. In light of the NRCs of the CV-treated OPB specimens (*i.e.* > 0.4), the convection drying technology is operationally and economically suited to the high-performance sound absorption oil palm boards (OPB). Specifically, the ideal convection-drying condition was 100 °C (Table 3). However, such is not the case with the microwave drying scheme as the NRCs are below the 0.4 threshold.

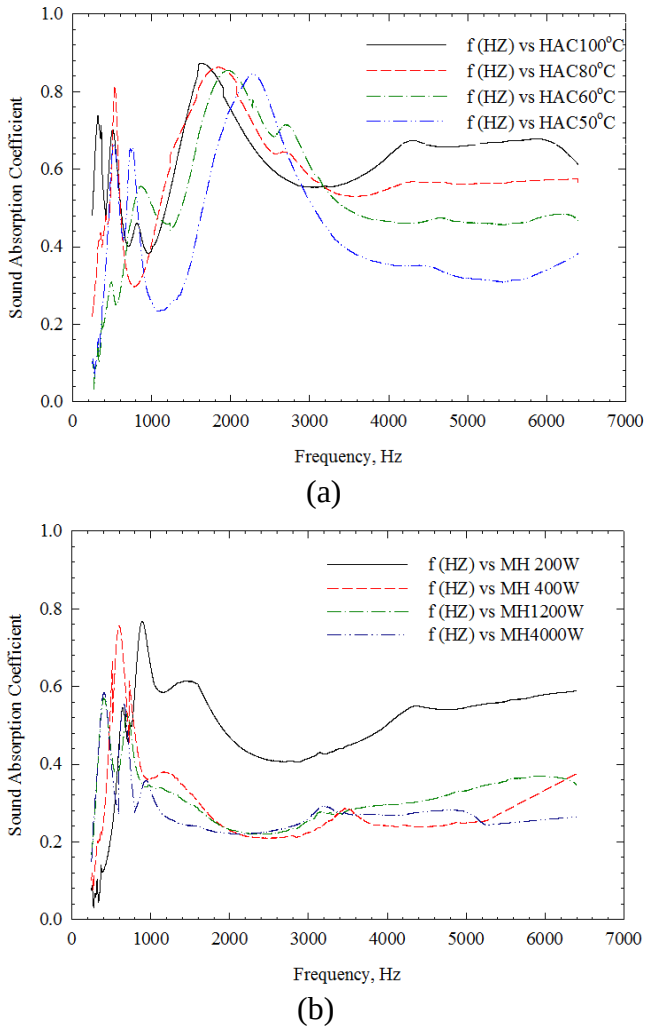

Fig. 8. The SAC of the OPB specimens treated with: (a) convection drying schemes (b) microwave drying schemes

Table 3. Maximum Sound Absorption Coefficients (SAC) at Various Frequencies and Noise Reduction Coefficients (NRC) of the CV- and MW-Treated OPB Specimens under Variable Thermal Conditions

Drying Treatment		Maximum SAC @ Frequency	Noise Reduction Coefficient (NRC)
Convection	50 °C	0.87; 1624 Hz	0.44
	60 °C	0.86; 1830 Hz	0.45
	80 °C	0.85; 1961 Hz	0.52
	100 °C	0.84; 2277 Hz	0.58
Microwave	200 W	0.76;894 Hz	0.35
	400 W	0.75;599 Hz	0.32
	1200 W	0.56;405 Hz	0.29
	4000 W	0.55;412 Hz	0.28

CONCLUSIONS

1. Under both the CV and MW schemes, oven temperatures were positively correlated with moisture desorption but inversely correlated with drying time. By comparison, the drying periods of the MW scheme were considerably shorter than those of the CV scheme. This was attributed to internal heat generation as a result of MW-induced mass transfer and subsequent rapid moisture desorption. In addition, given the high moisture content of the OPB specimens, the microwave energy was effectively absorbed and converted into sensible heat.
2. Under the CV drying scheme, heating temperatures were inversely correlated with oven-dry density and positively associated with volumetric shrinkage. Specifically, higher oven temperatures contributed to faster desorption rates, lower density, and higher volumetric shrinkage. The MW power output was positively correlated with oven-dry density and volumetric shrinkage of the OPB specimens as the moisture desorption was substantially accelerated as a result of MW-induced mass transfer and subsequent internal heat generation.
3. Under the CV scheme, the tension strength perpendicular to grain, compression strength parallel to grain, shear strength parallel to grain, static bending, and hardness decreased as the hot-air temperatures increased. In contrast, under the MW scheme, the mechanical strength increased with increasing MW power outputs, consistent with the increased shrinkage and density as the MW power increased. By comparison, the MW-treated OPB specimens exhibited stronger mechanical characteristics than those of the convection scheme.
4. As hot-air temperatures increased, the SEM images showed an abundance of fissures between the vascular bundles and parenchyma cells of the CV-treated OPB specimens. In contrast, no fissures emerged in the MW-treated OPB specimens as microwave power output increased. In fact, the vascular bundles and parenchyma cells became denser as MW power output increased.
5. The CV-treated OPB specimens acoustically outperformed the MW-treated counterparts as evidenced by the former's higher noise reduction coefficients (NRC) under all experimental thermal conditions. This phenomenon could be attributed to the abundance of fissures between the vascular bundles and the parenchyma in the CV-treated OPB specimens, which in turn contributed to better sound absorption performance.
6. Given the NRCs of the CV-treated OPB specimens (*i.e.* > 0.4), the convection drying technology is operationally and economically suited to the high-quality and high-performance acoustic OPB. Moreover, the ideal convection-drying condition is 100 °C. However, due to its lower NRC values (< 0.4), the microwave drying option is less operationally and economically viable.

ACKNOWLEDGMENTS

The authors would like to extend deep gratitude to the Office of the National Research Council of Thailand (NRCT) and King Mongkut's Institute of Technology

Ladkrabang (KMITL) for their financial assistance. Sincere appreciation also goes to Thammasat University's Research Center of Microwave Utilization in Engineering for their technical assistance in the analysis of the microwave-treated oil palm woods.

REFERENCES CITED

Abdul Khalil, H. P. S., Amouzgar, P., Jawaid, M., Abdullah, C. K., Issam, A. M., Zainudin, E. S., Paridah, M. T., and Hassan A. (2012). "Physical and thermal properties of microwave-dried wood lumber impregnated with phenol formaldehyde resin," *Journal of Composite Materials* 47(28), 3565-3571. DOI: 10.1177/0021998312467386

Abdullah, C. K., Jawaid, M., Abdul Khalil, H. P. S., Zaidon, A., and Hadiyane, A. (2012). "Oil palm trunk polymer composite: Morphology, water absorption, and thickness swelling behaviours," *BioResources* 7(3), 2948-2959. DOI: 10.15376/biores.7.3.2948-2959

Amouzgar, P., Abdul Khalil, H. P. S., Salamatinia, B., Abdullah, A. Z., and Issam, A. M. (2010). "Optimization of bioresource material from oil palm trunk core drying using microwave radiation; a response surface methodology application," *Bioresource Technology* 101(21), 8396-8401. DOI: 10.1016/j.biortech.2010.05.061

Arenas, J. P. and Crocker, M. J. (2010). "Recent trends in porous sound-absorbing materials," *Sound and Vibration* 44, 12-17.

Asdrubali, F. (2006). "Survey on the acoustical properties of new sustainable materials for noise control," *Euronoise* (30), 30 May-1 June 2006, Tampere, Finland.

Bhattacharya, I., Chakraborty, R., and Chowdhury, R. (2014). "Intensification of freeze-drying rate of Bacillus subtilis MTCC 2396 using tungsten halogen radiation: Optimization of moisture content and α-amylase activity," *Drying Technology* 32(7), 801-812. DOI: 10.1080/07373937.2013.860459

Choon, K. K., Killmann, W., Choon, L. S., Mansor, H., Utilization, K., Shaari, K. C., and Khoo, A. R. M. A. (1991). *Characteristics of the Oil Palm Stem*, Forest Research Institute Malaysia, Malaysia, pp.15-28.

Cowan, J. P. (1994). *Handbook of Environmental Acoustics*, Wiley Publishing, Hoboken, NJ, USA.

Du, G., Wang, S., and Cai, Z. (2005). "Microwave drying of wood strands," *Drying Technology* 23, 1-16.

Elustondo, D., Avramidis, S., and Shida, S. (2004). "Predicting thermal efficiency in timber radio frequency vacuum drying," *Drying Technology* 22(4), 795-807. DOI: 10.1081/DRT-120034263

Erwinsyah. (2008). *Improvement of Oil Palm Wood Properties using Bioresin*, Ph.D. Dissertation, Technische Universität Dresden, Dresden, Germany.

Feng, H., Tang, J., Cavalier, R. P., and Plumb, O. A. (2001). "Heat and mass transport in microwave drying of porous materials in a spouted bed," *AIChE Journal* 47(7), 1499-1512. DOI: 10.1002/aic.690470704

Fouladi, M. H., Ayub, M., and Nor, M. J. M. (2011). "Analysis of coir fiber acoustical characteristics," *Applied Acoustics* 72(1), 35-42. DOI: 10.1016/j.apacoust.2010.09.007

Hng, P. S., Wong, L. J., Chin, K. L., Tor, E. S., Tan, S. E., Tey, B. T., and Maminski, M. (2011). "Oil palm (*elaeis guineensis*) trunk as a resource of starch and other sugars," *Journal of Applied Sciences* 11(16), 3053-3057. DOI: 10.3923/jas.2011.3053.3057

Ismail, L., Ghazali, M. I., Mahzan S., and Zaidi, A. M. A. (2010). "Sound absorption of *Arenga pinnata* fiber," *International Journal of Chemical, Molecular, Nuclear, Materials and Metallurgical Engineering* 4(7), 438-440.

Johari, A., Nyakuma, B. B., Nor, S. H. M., Mat, R., Hashim, H., Ahmad, A., Zakaria, Z. Y., and Abdullah, T. A. T. (2015). "The challenges and prospects of palm oil based biodiesel in Malaysia," *Energy* 81, 255-261. DOI: 10.1016/j.energy.2014.12.037

Jung, H. S., Eom, C. D., and So, B. J. (2004). "Comparison of vacuum drying characteristics of radiata pine timber using different heating methods," *Drying Technology* 22(5), 1005-1022. DOI: 10.1081/DRT-120038577

Kerdtongmee, P., Saleh, A., Eadkhong, T., and Danworaphong, S. (2016). "Investigating sound absorption of oil palm trunk panels using one-microphone impedance tube," *BioResources* 11(4), 8409-8418. DOI: 10.15376/biores.11.4.8409-8418

Lai, L. W., and Idris, A. (2013). "Disruption of oil palm trunks and fronds by microwave-alkali pretreatment," *BioResources* 8(2), 2792-2804. DOI: 10.15376/biores.8.2.2792-2804

Langrish, T. A. G. (2013). "Comparing continuous and cyclic drying schedules for processing hardwood timber: The importance of mechanosorptive strain," *Drying Technology* 31(10), 1091-1098. DOI: 10.1080/07373937.2013.769449

Lars, H. (2007). *Microwave Treatment of Wood,* Doctoral Thesis, Luleå University of Technology, Skellefteå, Sweden.

Latif, H. A., Yahya, M. N. B., Rafig, M. N., and Hatta, M. N. M. (2015). "A preliminary study on acoustical performance of oil palm mesocarp natural fiber," *Applied Mechanics and Materials* 773-774, 247-252. DOI: 10.4028/www.scientific.net/AMM.773-774.247

Moreno, L. P., and Romero, H. M. (2015). "Phenology of the reproductive development of *Elaeis oleifera* (Kunth) cortes," *Agronomía Colombiana* 33(1), 36-42. DOI: 10.15446/agron.colomb.v33n1.47199

Nadhari, W. N. A. W., Hashim, R., Sulaiman, O., Sato, M., Sugimoto, T., and Selamat, M. E. (2013). "Utilization of oil palm trunk waste for manufacturing of binderless particleboard: Optimization study," *BioResources* 8(2), 1675-1696. DOI: 10.15376/biores.8.2.1675-1696

Norralakmam, S. Y. (2007). "Particleboards," in: *Turning Oil Palm Residues into Products (Research Pamphlets No.127),* Forest Research Institute Malaysia (FRIM), Kepong, Malaysia.

Or, K. H., Putra, A., Nor, M. J. M., Selamat, M. Z., and Ying, L. Z. (2016). "Sound absorption performance of oil palm empty fruit bunch fibers," 23rd International Congress on Sound & Vibration," The 23rd International Congress of Sound and Vibration, ICSV23, Athens (Greece)

Or, K. H., Putra, A., and Selamat, M. Z. (2017). "Oil palm empty fruit bunch fibres as sustainable acoustic absorber," *Applied Acoustics* 119, 9-16. DOI: 10.1016/j.apacoust.2016.12.002.

Ouertani, S., Hassini, L., Azzouz, S., Torres, S. S., Belghith, A., and Koubaa, A. (2015). "Modeling of combined microwave and convective drying of wood: Prediction of mechanical behavior via internal gas pressure," *Drying Technology* 33(10), 1234-1242. DOI: 10.1080/07373937.2015.1022828

Potts, J., Lynch, M., Wilkings, A., Huppé, G. A., Cunningham, M., and Voora, V. (2014). *The State of Sustainability Initiatives Review 2014 Standards and the Green Economy*, IISD, Manitoba, Canada.

Sa′adon, A. Z. M. (2015). "Utilization of oil palm trunk (*Elaeis guineensis*) as foam composite for sound absorption," *Jurnal Teknologi (Sciences & Engineering)* 77(32) 75-82.

Sanderson, K. (2011). "Lignocellulose: A chewy problem," *Nature* 474(7352), 12-14.DOI: 10.1038/474S012a

Schwarz, H. G. (1985). "Cement-bonded boards in Malaysia," Proceedings of the. Fibre and particleboards bonded with inorganic binders, *Forest Products Research Society* USA, 91-93.

Subiyanto, B., Subyakto, and Kawai, S. (2002). "Zero-emission processes of oil palm utilization case study of oil palm mill in PT. Kertajaya Lebak Banten province," in: *Proceedings of the Fourth International Wood Science Symposium*, Serpong, Indonesia, pp. 305-311.

Sulaiman, O., Salim, N., Nordin, N. A., Hashim, R., Ibrahim, M., and Sato, M. (2012). "The potential of oil palm trunk biomass as an alternative source for compressed wood," *BioResources* 7(2), 2688-2706. DOI: 10.15376/biores.7.2.2688-2706

Teck, C. L. and Ong, C. L. (1985). "Particleboard from oil palm trunk," *PORIM Bulletin* 11, 99-108.

Vongpradubchai, S. and Rattanadecho, P. (2011). "Microwave and hot air drying of wood using a rectangular waveguide," *Drying Technology* 29(4), 451-460. DOI: 10.1080/07373937.2010.505312

Article submitted: July 9, 2017; Pere review completed: October 10, 2017; Revised version received and accepted: November 30, 2017; Published: December 6, 2017.
DOI: 10.15376/biores.13.1.929-944